XII International Conference on Computational Plasticity. Fundamentals and Applications
COMPLAS XII
E. Oñate, D.R.J. Owen, D. Peric and B. Suárez (Eds)

A THERMOVISCOPLASTIC MODEL WITH DAMAGE FOR SIMULTANEOUS HOT/COLD FORGING ANALYSIS

C. Bröcker*, A. Matzenmiller*

[1]Institute of Mechanics, Department of Mechanical Engineering, University of Kassel
Moenchebergstreet 7, 34125 Kassel, Germany
e-mail: {broecker,amat}@uni-kassel.de

Key words: thermoviscoplasticity, damage, rheological models, simultaneous hot/cold forming, validation

Abstract. A constitutive model is presented for simultaneous hot/cold forming processes of steels. The phenomenological material theory is based on an enhanced rheological model and accounts temperature dependently for nonlinear hardening, thermally activated recovery effects, an improved description of energy storage and dissipation during plastic deformations, and damage evolution as well. A thermomechanically consistent treatment of dissipative heating due to inelastic deformations, recovery processes and damage mechanisms is applied. The constitutive model is implemented into a commercial FE-code. The material parameters of the effective model response are identified for a low alloyed steel and validated by means of a simultaneous hot/cold forging process.

1 Introduction

Innovative metal forming technologies make use of inhomogeneous temperature distribution, e.g. in the case of the simultaneous hot/cold forging—see figure 1, where hot and cold forming are applied locally to the workpiece in one single process step [21]. Hence, the temperature dependency of steel may be advantageously used to archive high degrees of deformation at lower forming forces in heated parts of the workpiece, respectively, strain hardening and less thermally induced distortion in the cold formed areas, which allows for the reduction of process steps and production costs. From the viewpoint of computational modeling of such processes, a huge challenge lies in a sufficiently accurate description of the temperature dependent material behavior, i.e. nonlinear strain hardening, strain rate sensitivity, thermal softening and recovery processes as well as potentially

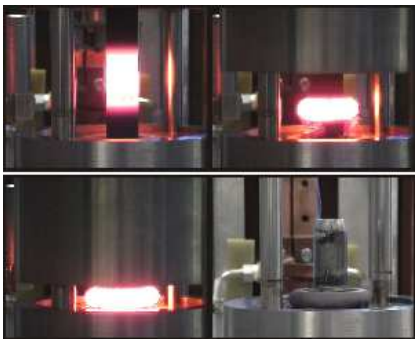

Figure 1: Simultaneous hot/cold forging process [21].

the detection and evolution of damage processes must be considered within the total relevant temperature range. However, the current state of art models—e.g. [9, 2, 11, 19]—fail to meet this demand.

The phenomenological material model, proposed for simultaneous hot/cold forging processes of steels, is based on an enhanced rheological model—see [5, 8], which contains new basics elements besides spring, dashpot and friction element to account for nonlinear hardening, and thermally activated recovery effects as well as an improved description of energy storage and dissipation during plastic deformations—see figure 2.

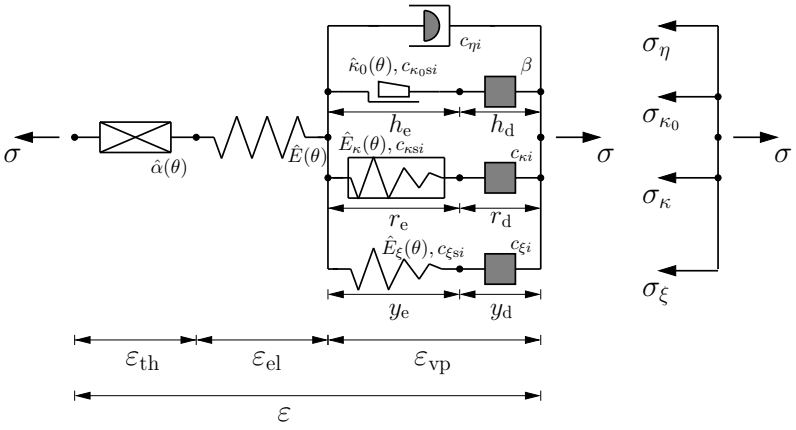

Figure 2: Rheological models of thermoviscoplasticity with nonlinear isotropic and kinematic hardening, temperature dependent material parameters and static recovery. Gray coloring of elements indicates dissipation of related stress power.

The thermoelastic contribution of the network[1] in figure 2 comprises a series connection of a thermal strain element with the thermal expansion coefficient $\hat{\alpha}(\theta)$ on the left hand side and a linear spring with the stiffness $\hat{E}(\theta)$ in the middle of the network. The temperature dependent viscoplastic part on the right hand side of the rheological model, however, consists of four chains arranged in parallel, each one representing a specific phenomenon of the entire elastoviscoplastic material response. The nonlinear dashpot (parameters $c_{\eta i}$) on top of the viscoplastic contribution is necessary to include nonlinear rate dependency. Below, the friction body is placed in connection with a novel dissipative strain element (with parameter β) in order to account for the initial yield limit $\hat{\kappa}_0(\theta)$ and to enhance the modeling capacity of energy storage and dissipation processes during plastic deformation. Next, a new hardening body with the stiffness $\hat{E}_\kappa(\theta)$ is put in series connection to another dissipative strain element (parameters $c_{\kappa i}$) in order to model nonlinear isotropic hardening. Finally, the arrangement of a linear spring with the stiffness $\hat{E}_\xi(\theta)$ and a third dissipative strain body (parameters $c_{\xi i}$) at the bottom of the viscoplastic network contribution represent nonlinear kinematic hardening. The stress power, which is spent at the friction and the hardening body as well as at spring of kinematic hardening, is stored in the network as free energy. Moreover, also static recovery is accounted for in these basic components (associated recovery parameters are $c_{\kappa 0 si}$,$c_{\kappa si}$,$c_{\xi si}$), which means that hardening diminishes and the related stored energy is released and dissipated as heat.

The rheological network directly provides the kinematics of the material model and

[1]Note, a spatial rheological model may be also represented graphically, which additionally accounts for an additive decomposition of the stress and the strain tensor into the spherical and the deviatoric contribution—see [5, 8] for more details.

the equilibrium of internal stresses for the viscoplastic network contribution. Moreover, these relations lead to the yield function $f = |\sigma - \xi| - (\hat{\kappa}_0(\theta) + \kappa) \geq 0$ and the flow rule $\dot{\varepsilon}_{\mathrm{vp}} = \lambda \frac{\sigma - \xi}{|\sigma - \xi|}$ by means of rearrangements in the framework of the balance equations of thermomechanics, where the plastic multiplier λ is calculated from the stress σ_η in the nonlinear dashpot. However, in lack of space, only the final material model is presented afterward in this paper. Hence, the interested reader is referred to [5, 8, 7] concerning the detailed procedure for deducing the constitutive equations from the rheological model.

The enhanced rheological model also allows for damage representation—see [6]. In the framework of continuum mechanics and thermomechanically consistent material modeling, the constitutive equations may be extensively deduced from the rheological network and fit into the concept of effective stresses of continuum damage mechanics [17]—see also figure 3. The strain equivalence holds for the the total and the internal strain measures, i.e. the strain responses of the effective and the damaged state of the model are equivalent. Moreover, in the special case of isothermal conditions, a linear relationship turns out between the actual nominal (damaged) and the effective (undamaged) model state, i.e. the following steps provide the final model response—see [6]:

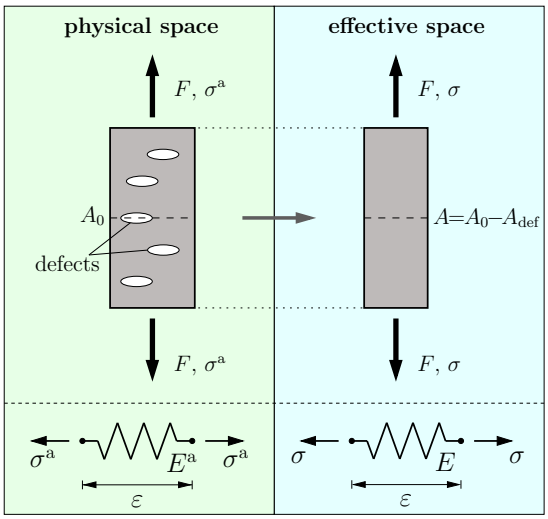

Figure 3: Sketch for motivation of the concept of effective stresses and its application for rheological models: σ denotes the effective stress and σ^{a} represents the actual nominal stress with damage.

1. Solve the effective material response without damage,
2. Determine the current damage state D from the evolution equation of damage,
3. Calculate the damaged state of the model by multiplying the total and internal effective stresses with the degradation/damage factor $(1 - D)$.

In general, however, there is a coupling between the effective and the nominal state of the model due to the temperature dependency of the material parameters and the dissipation of heat during the loading process.

In the next section, the constitutive model for simultaneous hot/cold forming is presented including some explanations concerning the implementation. Afterward, the model behavior is studied briefly. In the last section, the material parameters, identified for the effective part of the model, are verified by the test data and validated by means of the simultaneous hot/cold forming process in [21].

2 Thermoviscoplastic constitutive model with damage evolution

The proposed material theory is based on the rheological network in figure 2 and is formulated initially for small strains in the framework of thermomechanically consistent

material modeling—see e.g. [13]. The related free energy is assumed as—see also [10, 15]:

$$\psi^{\mathrm{a}} = \psi_{\mathrm{th}} + (1-D)\psi_{\mathrm{M}} \quad , \qquad \psi_{\mathrm{th}} = \hat{Q}(\theta)\,, \tag{1}$$

in which ψ_{th} denotes the purely temperature dependent part of the thermal strain element and ψ_{M} represent the mechanical contribution of the effective material model

$$\psi_{\mathrm{M}} = \frac{1}{2\rho}\left(2\hat{G}(\theta)\,\mathbf{E}_{\mathrm{el}}^{\mathsf{D}}\cdot\mathbf{E}_{\mathrm{el}}^{\mathsf{D}} + \hat{K}(\theta)\,\mathrm{tr}(\mathbf{E}_{\mathrm{el}})^2 + 2\hat{\kappa}_0(\theta)\,\varepsilon_{\kappa_0} + \hat{E}_{\kappa}(\theta)\,\varepsilon_{\kappa}^2 + \hat{E}_X(\theta)\,\mathbf{E}_X\cdot\mathbf{E}_X\right), \tag{2}$$

which is multiplied by the degradation factor $(1-D)$ with D as the scalar internal variable of damage. In (2), the mass density ρ is constant, while the shear modulus $\hat{G}(\theta)$, the bulk modulus $\hat{K}(\theta)$, the initial yield stress $\hat{\kappa}_0(\theta)$, and the stiffness parameter of isotropic $\hat{E}_{\kappa}(\theta)$ and kinematic hardening $\hat{E}_X(\theta)$ depend on the temperature. Moreover, $\mathbf{E}_{\mathrm{el}}$ is the elastic strain tensor, and $(\,)^{\mathsf{D}}$ as well as $\mathrm{tr}(\,)$ are the deviator and trace operators. In addition, ε_{κ_0} denotes an internal strain of the friction element to account for energy storage in this rheological component, whereas ε_{κ} and $\mathbf{E}_X$ are the internal strains of hardening belonging to the (isotropic) hardening body and the linear spring of kinematic hardening.

The stress $\mathbf{T}^{\mathrm{a}}$ in the damaged state of the material model is obtained according to[2]

$$\mathbf{T}^{\mathrm{a}} = \rho\frac{\partial\psi^{\mathrm{a}}}{\partial\mathbf{E}_{\mathrm{el}}} = (1-D)\,\mathbf{T} \quad , \qquad \mathbf{T} = \rho\frac{\partial\psi_{\mathrm{M}}}{\partial\mathbf{E}_{\mathrm{el}}} = 2\,\hat{G}(\theta)\,\mathbf{E}_{\mathrm{el}}^{\mathsf{D}} + \hat{K}(\theta)\,\mathrm{tr}(\mathbf{E}_{\mathrm{el}})\;\mathbf{1}\,, \tag{3}$$

while $\mathbf{T}$ is the stress tensor of the effective model response. The yield function results for the nominal and the effective state of the model as

$$F^{\mathrm{a}} = (1-D)\,F \quad , \qquad F = \sqrt{3/2}\,\left\|\mathbf{T}^{\mathsf{D}} - \mathbf{X}\right\| - (\hat{\kappa}_0(\theta) + \kappa) \tag{4}$$

with the stresses of kinematic hardening $\mathbf{X}$ (also denoted as back stress) and isotropic hardening κ as well as the norm $\|\mathbf{A}\| = \sqrt{\mathbf{A}\cdot\mathbf{A}}$. The flow rule reads

$$\dot{\mathbf{E}}_{\mathrm{vp}} = \lambda\;\mathbf{N}\big(\mathbf{T}^{\mathsf{D}} - \mathbf{X}\big) \quad , \qquad \lambda = \frac{1}{\hat{\eta}(\theta)}\left\langle\frac{F}{\hat{D}(\kappa,\theta)}\right\rangle^{\hat{m}(\theta)}, \tag{5}$$

where the operator $\mathbf{N}(\mathbf{A}) = \frac{\mathbf{A}}{\|\mathbf{A}\|}$ gives the "direction" of a tensor. The stress of isotropic hardening follows from the free energy (2) according to

$$\kappa^{\mathrm{a}} = \rho\frac{\partial\psi^{\mathrm{a}}}{\partial\varepsilon_{\kappa}} = (1-D)\,\kappa \quad , \qquad \kappa = \rho\frac{\partial\psi_{\mathrm{M}}}{\partial\varepsilon_{\kappa}} = \hat{E}_{\kappa}(\theta)\,\varepsilon_{\kappa}\,. \tag{6}$$

The evolution equation of the conjugated internal strain ε_{κ} is chosen as—see [6, 5, 8]:

$$\dot{\varepsilon}_{\kappa} = \left(1 - \left(\frac{\varepsilon_{\kappa}}{\varepsilon_{\kappa}^{\infty}}\right)^{n_{\kappa}}\right)\dot{\mathrm{E}}_{\mathrm{vp}} - \hat{\dot{\varepsilon}}_{\kappa\mathrm{s}}^{*}(\theta)\left(\frac{\varepsilon_{\kappa}}{\varepsilon_{\kappa}^{\infty}}\right)^{n_{\kappa\mathrm{s}}}, \tag{7}$$

[2]Note that the upper index $^{\mathrm{a}}$ is used to indicate values in the damaged state of the model in order to distinguish them from their effective counterparts.

in which the first summand is related to nonlinear strain hardening with $\dot{\bar{\mathrm{E}}}_{\mathrm{vp}} = \sqrt{2/3}\,\|\dot{\mathbf{E}}_{\mathrm{vp}}\|$ and the second term represents thermally activated recovery processes. The parameter $\varepsilon_\kappa^\infty$ denotes the saturation value of the internal strain ε_κ. Moreover, n_κ and $n_{\kappa\mathrm{s}}$ are positive exponents and $\hat{\dot{\varepsilon}}^*_{\kappa\mathrm{s}}(\theta)$ is a non-negative temperature dependent recovery parameter. Hence, with the definition of the saturation value $\hat{\kappa}^\infty(\theta) = \hat{E}_\kappa(\theta)\,\varepsilon_\kappa^\infty$ of the effective stress of isotropic hardening κ, its evolution equation turns out similar as in [2, 19]:

$$\dot{\kappa} = \hat{E}_\kappa(\theta)\left[\left(1 - \left(\frac{\kappa}{\hat{\kappa}^\infty(\theta)}\right)^{n_\kappa}\right)\dot{\bar{\mathrm{E}}}_{\mathrm{vp}} - \hat{\dot{\varepsilon}}^*_{\kappa\mathrm{s}}(\theta)\left(\frac{\kappa}{\hat{\kappa}^\infty(\theta)}\right)^{n_{\kappa\mathrm{s}}}\right] + \frac{\partial_\theta \hat{E}_\kappa(\theta)}{\hat{E}_\kappa(\theta)}\,\kappa\,\dot{\theta}\,, \tag{8}$$

with $\partial_\theta \hat{E}_\kappa(\theta)$ denoting the partial derivative of $\hat{E}_\kappa(\theta)$ with respect to the temperature θ. The stresses of kinematic hardening (back stresses) are obtained from (2) according to

$$\mathbf{X}^{\mathrm{a}} = \rho\frac{\partial \psi^{\mathrm{a}}}{\partial \mathbf{E}_X} = (1-D)\,\mathbf{X} \quad , \qquad \mathbf{X} = \rho\frac{\partial \psi_{\mathrm{M}}}{\partial \mathbf{E}_X} = \hat{E}_X(\theta)\,\mathbf{E}_X\,. \tag{9}$$

The evolution of the associated back strains is defined with a similar structure as in (7):

$$\dot{\mathbf{E}}_X = \dot{\mathbf{E}}_{\mathrm{vp}} - \left(\frac{\|\mathbf{E}_X\|}{\varepsilon_X^\infty}\right)^{n_X}\mathbf{N}(\mathbf{X})\,\dot{\bar{\mathrm{E}}}_{\mathrm{vp}} - \hat{\dot{\varepsilon}}^*_{X\mathrm{s}}(\theta)\left(\frac{\|\mathbf{E}_X\|}{\varepsilon_X^\infty}\right)^{n_{X\mathrm{s}}}\mathbf{N}(\mathbf{E}_X)\,, \tag{10}$$

in which the directions $\mathbf{N}(\mathbf{X})$ and $\mathbf{N}(\mathbf{E}_X)$ in the second and third summand ensure the thermomechanical consistency of this approach. All the related material parameters have the same meaning as before in the case of isotropic hardening. Hence, with the saturation value $\hat{X}^\infty(\theta) := \hat{E}_X(\theta)\,\varepsilon_X^\infty$ of the norm $\|\mathbf{X}\|$, the evolution equation of kinematic hardening in the effective state turns out as

$$\dot{\mathbf{X}} = \hat{E}_X(\theta)\left[\dot{\mathbf{E}}_{\mathrm{vp}} - \left(\frac{\|\mathbf{X}\|}{\hat{X}^\infty(\theta)}\right)^{n_X}\mathbf{N}(\mathbf{X})\,\dot{\bar{\mathrm{E}}}_{\mathrm{vp}} - \hat{\dot{\varepsilon}}^*_{X\mathrm{s}}(\theta)\left(\frac{\|\mathbf{X}\|}{\hat{X}^\infty(\theta)}\right)^{n_{X\mathrm{s}}}\mathbf{N}(\mathbf{X})\right] + \frac{\partial_\theta \hat{E}_X(\theta)}{\hat{E}_X(\theta)}\,\mathbf{X}\,\dot{\theta}\,. \tag{11}$$

The experimental characterization of energy storage and dissipation during plastic flow of metals reveal that at the beginning of loading, much plastic work is stored in the material—see e.g. [3]. However, current state of art plasticity models usually underestimate such energy storage phenomena. Hence, additional energy storage is related to the friction element, besides the common storage mechanism of energy due to hardening—see in particular [5, 8]. The associated internal strain variable is defined according to—see [8]

$$\dot{\varepsilon}_{\kappa 0} = \hat{\beta}(\theta)\left(1 - \left(\frac{\varepsilon_\kappa}{\varepsilon_\kappa^\infty}\right)^{n_\kappa}\right)\dot{\bar{\mathrm{E}}}_{\mathrm{vp}} - \hat{\dot{\varepsilon}}^*_{\kappa\mathrm{s}}(\theta)\left(\frac{\varepsilon_{\kappa 0}}{\varepsilon_\kappa^\infty}\right)^{n_{\kappa\mathrm{s}}}\,, \tag{12}$$

which is the generalization of an approach from [5] for temperature dependency and static recovery. The definitions of all temperature dependent parameters specified above may be found in [8] and, for the uniaxial case without energy storage in the friction body, also in [6].

Damage evolution

The evolution of the scalar internal variable of damage is chosen similar to the approach in [14] in the first step—see also [6]:

$$D = \left\langle \frac{\bar{\mathrm{E}}_{\mathrm{vp}} - \hat{\varepsilon}_{\mathrm{c0}}}{\hat{\varepsilon}_{\mathrm{f0}} - \hat{\varepsilon}_{\mathrm{c0}}} \right\rangle^{n_{\mathrm{D}}} \quad \Rightarrow \quad \dot{D} = \frac{n_{\mathrm{D}}}{\varepsilon_{\mathrm{f0}} - \varepsilon_{\mathrm{c0}}} \left\langle \frac{\bar{\mathrm{E}}_{\mathrm{vp}}/\hat{g}(\dot{\bar{\mathrm{E}}}, T, \theta) - \varepsilon_{\mathrm{c0}}}{\varepsilon_{\mathrm{f0}} - \varepsilon_{\mathrm{c0}}} \right\rangle^{n_{\mathrm{D}}-1} \frac{\dot{\bar{\mathrm{E}}}_{\mathrm{vp}}}{\hat{g}(\dot{\bar{\mathrm{E}}}, T, \theta)} , \quad (13)$$

in which $\bar{\mathrm{E}}_{\mathrm{vp}} = \sqrt{2/3} \int_0^t \|\dot{\mathbf{E}}_{\mathrm{vp}}\| \, \mathrm{d}\tau$ denotes the arclength of the viscoplastic strain rate and, furthermore, $\hat{\varepsilon}_{\mathrm{c0}} = \varepsilon_{\mathrm{c0}} \, \hat{g}(\dot{\bar{\mathrm{E}}}, T, \theta)$ and $\hat{\varepsilon}_{\mathrm{f0}} = \varepsilon_{\mathrm{f0}} \, \hat{g}(\dot{\bar{\mathrm{E}}}, T, \theta)$ represent the critical threshold values for damage initiation and the failure strain with the parameters $\varepsilon_{\mathrm{c0}} > 0$ and $\varepsilon_{\mathrm{f0}} > 0$ as well as the strain rate, temperature and stress dependent function $\hat{g}$ according to [14]:

$$\hat{g}(\dot{\bar{\mathrm{E}}}, T, \theta) = \Big(1 + d_2 \, \mathrm{e}^{(-d_3 T)}\Big)\Big(1 + d_4 \ln(\dot{\bar{\mathrm{E}}}/\dot{\varepsilon}_0)\Big)(1 + d_5 \theta) \, . \quad (14)$$

The parameters d_i are semipositive and the variable T is denoted as triaxiality and serves for characterizing the stress state during loading:

$$T = \frac{-\operatorname{tr}(\mathbf{T}^{\mathrm{a}})}{||\mathbf{T}^{\mathrm{aD}}||} = \frac{-\operatorname{tr}(\mathbf{T})}{||\mathbf{T}^{\mathrm{D}}||} \, , \quad (15)$$

since the hydrostatic pressure significantly influences damage evolution—see e.g. [14].

Equation of heat conduction and mechanical dissipation

The equation of heat conduction reads in a general formulation—cf. [13, 6]

$$\hat{c}^{\mathrm{a}}_{\mathrm{ed}} \, \dot{\theta} = \underbrace{-\theta \frac{\partial s^{\mathrm{a}}}{\partial \mathbf{E}_{\mathrm{el}}} \cdot \dot{\mathbf{E}}_{\mathrm{el}}}_{-p^{\mathrm{a}}_{\mathrm{te}}} + \underbrace{\frac{1}{\rho} \operatorname{div} \vec{q} + b}_{p_{\mathrm{Q}}} + \underbrace{\frac{1}{\rho} \mathbf{T}^{\mathrm{a}} \cdot \dot{\mathbf{E}}_{\mathrm{vp}} - \sum_{j=1}^{n} \frac{\partial \psi^{\mathrm{a}}}{\partial a_j} \dot{a}_j}_{\delta^{\mathrm{a}}_{\mathrm{M}}} \underbrace{- \theta \sum_{j=1}^{n} \frac{\partial s^{\mathrm{a}}}{\partial a_j} \dot{a}_j}_{-p^{\mathrm{a}}_{\mathrm{ti}}} , \quad (16)$$

in which $\hat{c}^{\mathrm{a}}_{\mathrm{ed}}$ is the natural heat capacity at constant elastic deformation and s^{a} the entropy:

$$\hat{c}^{\mathrm{a}}_{\mathrm{ed}} := \theta \, \frac{\partial \, s^{\mathrm{a}}(\mathbf{E}_{\mathrm{el}}, \theta, a_1, ..., a_n)}{\partial \theta} \quad , \qquad s^{\mathrm{a}} = \boldsymbol{\alpha} \cdot \frac{\partial \psi^{\mathrm{a}}}{\partial \mathbf{E}_{\mathrm{el}}} - \frac{\partial \psi^{\mathrm{a}}}{\partial \theta} = \frac{1}{\rho} \mathbf{T}^{\mathrm{a}} \cdot \boldsymbol{\alpha} - \frac{\partial \psi^{\mathrm{a}}}{\partial \theta} \, , \quad (17)$$

with $\boldsymbol{\alpha}$ as the tensor of the thermal expansion coefficient. Moreover, in (16), $p^{\mathrm{a}}_{\mathrm{te}}$ and $p^{\mathrm{a}}_{\mathrm{ti}}$ denote the thermoelastic and thermoinelastic coupling terms with $a_j = \{\varepsilon_{\kappa_0}, \varepsilon_{\kappa}, \mathbf{E}_X, D\}$. Furthermore, p_{Q} is assumed to be unaffected by damage and comprises heat conduction ($\vec{q}$

is the heat flux vector) and volumetric heat sources b. The summand $\delta^{\mathrm{a}}_{\mathrm{M}}$ is the mechanical dissipation power—see also [5]. The entropy is calculated from the free energy (2) as:

$$s^{\mathrm{a}} = \frac{1}{\rho}(1-D)\left(3\hat{K}(\theta)\,\hat{\alpha}(\theta)\;\mathrm{tr}(\mathbf{E}_{\mathrm{el}}) - \partial_\theta\,\hat{G}(\theta)\,\mathbf{E}^{\mathsf{D}}_{\mathrm{el}}\cdot\mathbf{E}^{\mathsf{D}}_{\mathrm{el}} - \frac{1}{2}\partial_\theta\,\hat{K}(\theta)\;\mathrm{tr}(\mathbf{E}_{\mathrm{el}})^2\right)$$
$$- \partial_\theta\,\hat{Q}(\theta) - \frac{1}{\rho}(1-D)\left(\partial_\theta\hat{\kappa}_0(\theta)\,\varepsilon_{\kappa_0} + \frac{1}{2}\partial_\theta\hat{E}_\kappa(\theta)\,\varepsilon_\kappa^2 + \frac{1}{2}\partial_\theta\hat{E}_X(\theta)\,\mathbf{E}_X\cdot\mathbf{E}_X\right). \tag{18}$$

Hence, the heat capacity at constant elastic deformation results to

$$\hat{c}^{\mathrm{a}}_{\mathrm{ed}} = -\theta\,\partial_{\theta\theta}\,\hat{Q}(\theta) + \frac{1}{\rho}(1-D)\,\theta\Big(3\,\partial_\theta\,\hat{K}(\theta)\,\hat{\alpha}(\theta)\;\mathrm{tr}(\mathbf{E}_{\mathrm{el}}) + 3\hat{K}(\theta)\,\partial_\theta\,\hat{\alpha}(\theta)\;\mathrm{tr}(\mathbf{E}_{\mathrm{el}})$$
$$- \partial_{\theta\theta}\,\hat{G}(\theta)\,\mathbf{E}^{\mathsf{D}}_{\mathrm{el}}\cdot\mathbf{E}^{\mathsf{D}}_{\mathrm{el}} - \frac{1}{2}\partial_{\theta\theta}\,\hat{K}(\theta)\,\mathrm{tr}(\mathbf{E}_{\mathrm{el}})^2\Big)$$
$$- \frac{1}{\rho}(1-D)\,\theta\Big(\partial_{\theta\theta}\,\hat{\kappa}_0(\theta)\,\varepsilon_{\kappa_0} + \frac{1}{2}\partial_{\theta\theta}\,\hat{E}_\kappa(\theta)\,\varepsilon_\kappa^2 + \frac{1}{2}\partial_{\theta\theta}\,\hat{E}_X(\theta)\,\mathbf{E}_X\cdot\mathbf{E}_X\Big) \tag{19}$$

and appears as a process dependent function of all the arguments of the free energy. The thermoelastic $p^{\mathrm{a}}_{\mathrm{te}}$ and the thermoinelastic coupling term $p^{\mathrm{a}}_{\mathrm{ti}}$ turn out as

$$p^{\mathrm{a}}_{\mathrm{te}} = (1-D)\,p_{\mathrm{te}} \quad , \qquad p^{\mathrm{a}}_{\mathrm{ti}} = p^{\mathrm{a}}_{\mathrm{tp}} + p^{\mathrm{a}}_{\mathrm{tD}} \quad , \qquad p^{\mathrm{a}}_{\mathrm{tp}} = (1-D)\,p_{\mathrm{tp}} \tag{20}$$

with their counterparts of the effective material model according to

$$p_{\mathrm{te}} = \frac{1}{\rho}\theta\left(\partial_\theta\hat{K}(\theta)\;\mathrm{tr}(\mathbf{E}_{\mathrm{el}})\,\mathbf{1} - 3\hat{K}(\theta)\,\hat{\alpha}(\theta)\,\mathbf{1} + 2\,\partial_\theta\,\hat{G}(\theta)\,\mathbf{E}^{\mathsf{D}}_{\mathrm{el}}\right)\cdot\dot{\mathbf{E}}_{\mathrm{el}}\,, \tag{21}$$

$$p_{\mathrm{tp}} = \frac{1}{\rho}\,\theta\left(\partial_\theta\hat{\kappa}_0(\theta)\,\dot{\varepsilon}_{\kappa_0} + \partial_\theta\hat{E}_\kappa(\theta)\,\varepsilon_\kappa\,\dot{\varepsilon}_\kappa + \partial_\theta\hat{E}_X(\theta)\,\mathbf{E}_X\cdot\dot{\mathbf{E}}_X\right). \tag{22}$$

Furthermore, the thermoinelastic coupling term $p^{\mathrm{a}}_{\mathrm{ti}}$ comprises an additional contribution $p^{\mathrm{a}}_{\mathrm{tD}}$ due to damage evolution:

$$p^{\mathrm{a}}_{\mathrm{tD}} = \frac{1}{\rho}\theta\left(3\hat{K}(\theta)\,\hat{\alpha}(\theta)\;\mathrm{tr}(\mathbf{E}_{\mathrm{el}}) - \partial_\theta\,\hat{G}(\theta)\,\mathbf{E}^{\mathsf{D}}_{\mathrm{el}}\cdot\mathbf{E}^{\mathsf{D}}_{\mathrm{el}} - \frac{1}{2}\partial_\theta\,\hat{K}(\theta)\;\mathrm{tr}(\mathbf{E}_{\mathrm{el}})^2\right)\dot{D}$$
$$- \frac{1}{\rho}\theta\left(\partial_\theta\hat{\kappa}_0(\theta)\,\varepsilon_{\kappa_0} + \frac{1}{2}\partial_\theta\hat{E}_\kappa(\theta)\,\varepsilon_\kappa^2 + \frac{1}{2}\partial_\theta\hat{E}_X(\theta)\,\mathbf{E}_X\cdot\mathbf{E}_X\right)\dot{D}\,. \tag{23}$$

In order to prove the thermomechanical consistency of the model, the mechanical dissipation $\delta^{\mathrm{a}}_{\mathrm{M}}$ is evaluated and separated into both semipositive summands:

$$\delta^{\mathrm{a}}_{\mathrm{M}} = \delta^{\mathrm{a}}_{\mathrm{vp}} + \delta^{\mathrm{a}}_{\mathrm{D}} \quad , \qquad \delta^{\mathrm{a}}_{\mathrm{vp}} = (1-D)\,\delta_{\mathrm{vp}} \geq 0 \quad , \qquad \delta^{\mathrm{a}}_{\mathrm{D}} = \psi_{\mathrm{M}}\dot{D} \geq 0\,. \tag{24}$$

The second part $\delta^{\mathrm{a}}_{\mathrm{D}}$ is due to damage evolution and represents the dissipation of the mechanical free energy (2), which has been stored in the material during the loading

process. The first summand, however, is the product of the degradation factor $(1-D)$ and the viscoplastic dissipation power of the effective material model δ_{vp}, which one again may be arranged into two expressions:

$$\delta_{\mathrm{vp}} = \frac{1}{\rho}\left[F + \Big(1-\hat{\beta}(\theta)\Big)\hat{\kappa}_0(\theta) + \Big(\beta(\theta)\,\hat{\kappa}_0(\theta) + \kappa\Big)\left(\frac{\kappa}{\hat{\kappa}^{\infty}(\theta)}\right)^{n_\kappa} + \|\mathbf{X}\|\left(\frac{\|\mathbf{X}\|}{\hat{X}^{\infty}(\theta)}\right)^{n_X}\right]\dot{\bar{\mathrm{E}}}_{\mathrm{vp}} + \frac{1}{\rho}\left[\left(\hat{\kappa}_0(\theta)\left(\frac{\varepsilon_{\kappa_0}}{\varepsilon^{\infty}_{\kappa}}\right)^{n_{\kappa\mathrm{s}}} + \kappa\left(\frac{\kappa}{\hat{\kappa}^{\infty}(\theta)}\right)^{n_{\kappa\mathrm{s}}}\right)\hat{\dot{\varepsilon}}^{*}_{\kappa\mathrm{s}}(\theta) + \|\mathbf{X}\|\left(\frac{\|\mathbf{X}\|}{\hat{X}^{\infty}(\theta)}\right)^{n_{X\mathrm{s}}}\hat{\dot{\varepsilon}}^{*}_{X\mathrm{s}}(\theta)\right] \geq 0\,. \tag{25}$$

Its first line represents the dissipation due to plastic loading and is associated to the dashpot and the three dissipative strain elements in the rheological network of figure 2. In contrast, the second line of (25) gives the dissipation of free energy due to static recovery in the friction and hardening body as well as in the spring of kinematic hardening.

Hypoelastoviscoplastic large-deformation formulation and implementation

Thanks to the ease of implementation in the standard non-linear FE-codes like LS-DYNA, the Jaumann stress rate $\mathring{\mathbf{T}}_J$ and the rate of deformation $\mathbf{D}$ are applied as the statical and dynamical variables for the rate constitutive model of finite deformation plasticity, although it is well-known that they are not energy conjugate stress and strain measures [18, 13]. However, due to the small elastic strain in the presence at finite deformations, this procedure may be justified in the limit of engineering precision.

The small-strain, hyperelastic material theory presented above my be easily converted into an objective finite-deformation rate-formulation on the current configuration under the assumptions of small elastic $\mathbf{E}_{\mathrm{el}}$ and small back strains $\mathbf{E}_X$ and an isotropic thermal expansion behavior—see e.g. [8] for more details. Thus, it holds for the strain rate tensor

$$\mathbf{D} = \mathbf{D}_{\mathrm{th}} + \mathbf{D}_{\mathrm{el}} + \mathbf{D}_{\mathrm{vp}} \quad , \qquad \mathbf{D}_{\mathrm{th}} = \hat{\alpha}(\theta)\,\dot{\theta}\,\mathbf{1} \quad , \qquad \mathbf{D}_{\mathrm{vp}} = \lambda\,\mathbf{N}\big(\mathbf{T}^{\mathsf{D}} - \mathbf{X}\big) \tag{26}$$

with the kinematical analogy between the strain measures of small and large deformations:

$$\dot{\mathbf{E}}_{\mathrm{el}} \mathrel{\widehat{=}} \mathbf{D}_{\mathrm{el}} \quad , \qquad \dot{\mathbf{E}}_{\mathrm{vp}} \mathrel{\widehat{=}} \mathbf{D}_{\mathrm{vp}} \quad , \qquad \dot{\bar{\mathrm{E}}}_{\mathrm{vp}} \mathrel{\widehat{=}} \bar{\mathrm{D}}_{\mathrm{vp}}\,. \tag{27}$$

A hypoelastic relation is assumed for the Cauchy stress according to

$$\mathring{\mathbf{T}}_J = 2\,\hat{G}(\theta)\,\mathbf{D}^{\mathsf{D}}_{\mathrm{el}} + \hat{K}(\theta)\,\mathrm{tr}(\mathbf{D}_{\mathrm{el}})\;\mathbf{1} + \left(\frac{\partial_\theta \hat{G}(\theta)}{\hat{G}(\theta)}\;\mathbf{T}^{\mathsf{D}} + \frac{\partial_\theta \hat{K}(\theta)}{\hat{K}(\theta)}\;\mathrm{tr}(\mathbf{T})\;\mathbf{1}\right)\dot{\theta} \tag{28}$$

and the evolution equation (11) of the back stress is rewritten as

$$\mathring{\mathbf{X}}_J = \hat{E}_X(\theta)\left[\mathbf{D}_{\mathrm{vp}} - \left(\frac{\|\mathbf{X}\|}{\hat{X}^{\infty}(\theta)}\right)^{n_X}\mathbf{N}(\mathbf{X})\,\bar{\mathrm{D}}_{\mathrm{vp}} - \hat{\dot{\varepsilon}}^{*}_{X\mathrm{s}}(\theta)\left(\frac{\|\mathbf{X}\|}{\hat{X}^{\infty}(\theta)}\right)^{n_{X\mathrm{s}}}\mathbf{N}(\mathbf{X})\right] + \frac{\partial_\theta \hat{E}_X(\theta)}{\hat{E}_X(\theta)}\,\mathbf{X}\,\dot{\theta}\,, \tag{29}$$

in which $\mathring{\mathbf{T}}_J$ and $\mathring{\mathbf{X}}_J$ denote the objective JAUMANN rates of the CAUCHY and the back stress. Note that the latter one approximately operates on the current configuration, too.

The material model is implemented into the finite element program LS-DYNA as a user subroutine. LS-DYNA uses a "staggered" solution strategy for the coupled field problem of the balance of momentum and the equation of heat conduction, i.e. the both field equations are solved separately one after the other. Hence, the mechanical time steps remain isothermal and, hence, in the user material model, the response of the effective material model must only be multiplied with the damage factor $(1 - D)$ to account for damage evolution. For the thermal time step, however, the equation of heat conduction is simplified as usually by means of the assumptions that both thermomechanical coupling terms are negligible and that the heat capacity is a function of the temperature only, i.e. $p_{\mathrm{te}} := 0$, $p_{\mathrm{tp}} := 0$ and $\hat{c}_{\mathrm{ed}} = \hat{c}_{\mathrm{ed}}(\theta)$ hold.

3 Simulation of uniaxial tension tests

The model capabilities are studied by means of the simulation of uniaxial tension tests with the program Matlab. The material parameters are chosen to represent a typical steel behavior. Figure 4 (left side) shows the flow curves with the nominal stress response colored and the effective stresses in gray. The related evolution of temperature is given in the right diagram, where, for the purpose of comparison, the temperature course is added in gray for an additional simulation without damage evolution.

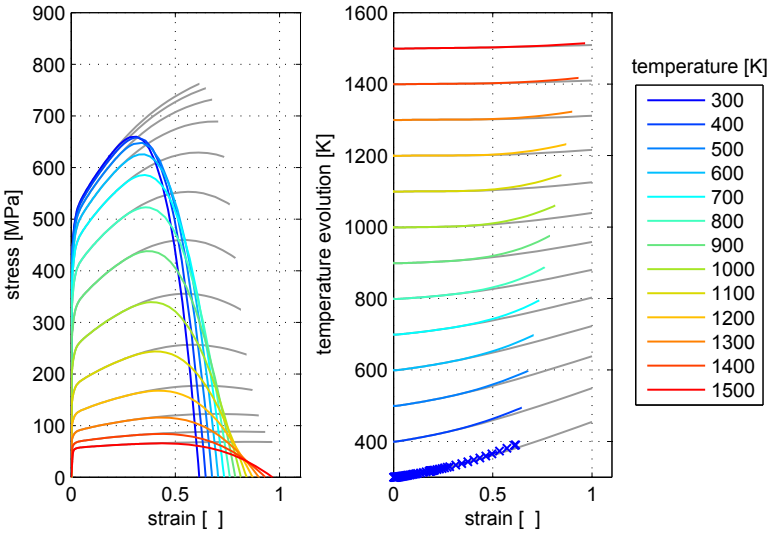

Figure 4: Matlab simulation of tension tests. Left: stress response (with effective stresses in gray). Right: evolution of temperature (with results of comparative calculation without damage in gray).

After a certain process dependent, critical equivalent strain value, the colored stress responses obviously diminish due to damage evolution in the material and finally drop to zero—see figure 4 (left). Note that some of the corresponding graphs of effective stresses (without damage) in gray also exhibit a slight decrease of the stress values at large strains, however, due to adiabatic heating and the associated thermal softening of the material.

The graphs of the simulated temperature courses in figure 4 (right) reveal the influence of damage evolution onto the adiabatic heating. In particular in the middle temperature range, the dissipative heating is significantly stronger due to damage evolution than in the gray graphs from the comparative calculation without any damage mechanisms.

4 Verification and validation of effective material model

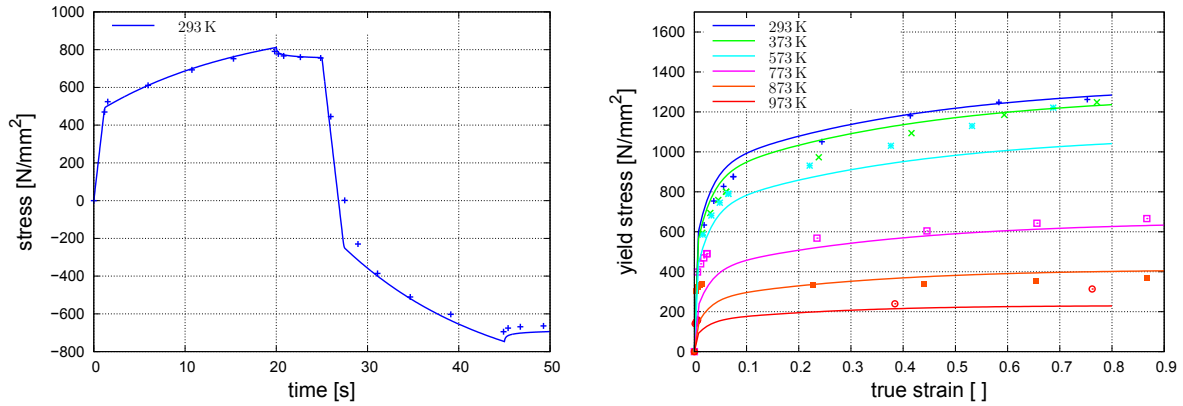

Figure 5: Comparison of test data (points) and simulation results (lines). Left: Tension-compression test with relaxation phases [1]. Right: Flow curves[3].

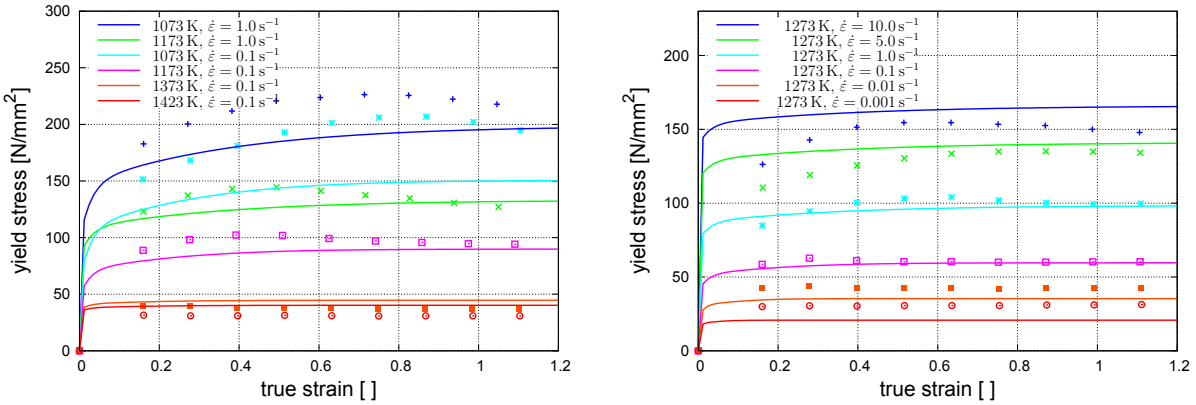

Figure 6: Comparison of experimental flow curve [12] (points) and simulation results (lines).

The material parameters of the effective part of the model are identified for the low alloyed steel 51CrV4 with the optimization program LS-OPT by means of test data at various temperature levels—see [8] for more details and the parameter listing. Figures 5–7 show the comparison between the experimental data and the related prediction with the identified material parameters. It may be summarized that the constitutive theory captures well the thermal dependency of the steel alloy 51CrV4 in the wide range of strain, strain rate and temperature.

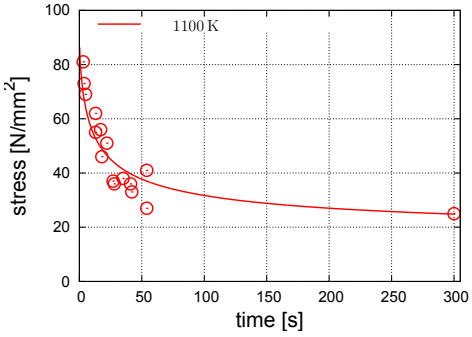

Figure 7: Comparison of recovery test data [16] (points) and simulation (lines).

Finally, the effective (undamaged) state of the model is validated briefly by means of the simultaneous hot/cold forging process in [21]—see figure 8. A detailed description

[3]The test data is kindly provided by Prof. Scholtes, Institute of Materials Engineering, University of Kassel, Kassel/Germany—see also [8].

about the modeling steps of this complex forming process with LS-DYNA may be found in [20, 8]. The proposed material theory is applied in a finite element simulation (FEM) as well as in a second analysis with element-free GALERKIN-Method (EFG)—see also [8]. Additionally, figure 8 presents the simulation results of the numerical study in [20], for which a standard plasticity model of LS-DYNA with a tabular based definition of the temperature and rate dependent yield stress. The proposed model yields better results than the standard plasticity model of LS-DYNA and enables are quite well prediction of the final geometry and the forming force of the forging process at hand as figure 8 reveals.

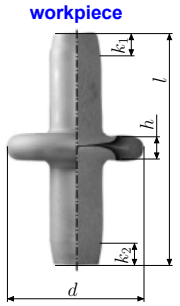

Label	Experiment (mm)	Simulation (mm)		
Model		Std-M	New-Model	
Analysis		FE	FE	EFG
k_1	12.0	13.9	13.3	12.7
k_2	14.0	13.9	13.3	12.6
h	13.6	13.5	13.6	13.7
d	76.8	78.1	77.8	77.6
l	130.6	131.3	130.3	129.0

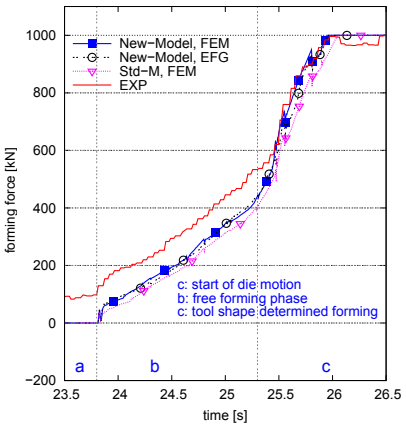

Figure 8: Comparison of test data[4] and simulation results of standard material model ("Std-M") of LS-DYNA [20] and proposed material theory.

5 Summary

A thermoviscoplasticity theory with damage is presented for simultaneous hot/cold forming, which is based on an enhanced rheological model. The constitutive equations are implemented into a commercial FE-code. The material theory captures the thermal dependency in the wide range from room temperature nearly up to the melting point. The material parameters of the effective model response are identified for a low alloyed steel and validated by means of a simultaneous hot/cold forging process.

Acknowledgment: The authors thankfully acknowledge the financial support of the German Research Foundation (DFG) through grant number Ma1186/5.

REFERENCES

[1] Al-Baldawi, A.: Identifikation der Materialparameter eines viskoelastisch-plastisches Materialmodells anhand experimenteller Daten aus einaxialen Versuchen: Vergleich von drei verschiedenen Chargen von 51CrV4. Diploma thesis at the Institute of Mechanics, University of Kassel, Germany (2009).

[4]The experimental data is kindly provided by Prof. Steinhoff, Institute of Production Technology and Logistics, Chair of Metal Forming Technology, University of Kassel, Kassel/Germany.

[2] Bammann, D.J.: Modeling temperature and strain rate dependent large deformations of metals. *Appl. Mech. Rev.*, 43, No. 5 Part 2 (1990), S312–S319.

[3] Bever, M.B., Holt, D.L., Titchener, A.L.: The Stored Energy of Cold Work, Pergamon Press (1973).

[4] Bröcker, C., Matzenmiller, A.: Thermoviscoplasticity deduced from enhanced rheological models. *PAMM*, Issue 1 (2012), 327–328.

[5] Bröcker, C., Matzenmiller, A.: An enhanced concept of rheological models to represent nonlinear thermoviscoplasticity and its energy storage behavior, *Continuum Mechanics and Thermodynamics*, DOI: 10.1007/s00161-012-0268-3 (2012).

[6] Bröcker, C., Matzenmiller, A.: Thermomechanically consistent material modeling with damage for simultaneous hot/cold forming based on enhanced rheological models, In: J. Eberhardsteiner et. al. (eds.): Proc. of European Congress on Computational Methods in Applied Sciences and Engineering (ECCOMAS 2012), Vienna, 10-14.09.2012.

[7] Bröcker, C., Matzenmiller, A.: 3D-generalization of the enhanced concept of rheological models to represent nonlinear thermoviscoplasticity. To be submitted to *Continuum Mechanics and Thermodynamics* (2013).

[8] Bröcker, C.: Materialmodellierung für die simultane Kalt-/Warmumformung auf Basis erweiterter rheologischer Modelle. Doctoral thesis submitted for examination, Institute of Mechanics, University of Kassel, Moenchebergstr. 7, Kassel (2013).

[9] Brown, S.B., Kim, K.H., Anand, L.: An internal variable constitutive model for hot working of metals, *Int. J. of Plasticity*, 5 (1989), 95–130.

[10] Grammenoudis, P., Reckwerth, D., Tsakmakis, C.: Continuum Damage Models based on Energy Equivalence: Part I Isotropic Material Response. *Int. J. of Damage Mechanics*, 18 no. 1 (2009), 31–63.

[11] Guo, Y.B., Wen, Q., Horstemeyer, M.F.: An internal state variable plasticity-based approach to determine dynamic loading history effects on material property in manufacturing processes. *Int. J. of Mechanical Sciences*, 47, No. 9 (2005), 1423–1441.

[12] Hagen, M.: Werkstoffmodelle zur thermomechanischen Behandlung des Stahls 50 CrV 4, PhD Thesis, RWTH Aachen, Aachen/Germany (1990).

[13] Haupt, P.: Continuum mechanics and theory of materials (Springer, Berlin, 2002).

[14] Johnson, G.R., Cook, W.H.: Fracture Characteristics of Three Metals Subjected to Various Strains, Strain Rates, Temperatures and Pressures. *Int. J. Fract. Mech.*, 21 (1985), 31–48.

[15] Kintzel, O., Mosler, J.: A coupled isotropic elasto-plastic damage model based on incremental minimization principles. *Technische Mechanik*, 30, Issues 1-3 (2010), 177–184.

[16] Lackowski, B., Lippmann, S.: Entfestigungsverhalten des Stahls 50CrV4 bei der thermomechanischen Behandlung, Mat.-wiss. u. Werkstofftech. **23** (1992), 145–150.

[17] Lemaitre, J., Chaboche, J.-L.: Mechanics of Solid Materials. Cambridge University Press, Cambridge (1990).

[18] Macvean, D.B.: Die Elementarbeit in einem Kontinuum und die Zuordnung von Spannungs- und Verzerrungstensoren, ZAMP, **19** (1968) 157-185

[19] Marin, E.B., Bammann, D.J., Regueiro, R.A., Johnson, G.C.: On the Formulation, Parameter Identification and Numerical Integration of the EMMI Model: Plasticity and Isotropic Damage. Sandia Report SAND2006-0200, Sandia National Laboratories, California, USA (2006).

[20] Matzenmiller, A., Bröcker, C.: Thermo-mechanically coupled FE analysis and sensitivity study of simultaneous hot/cold forging process with local inductive heating and cooling. *Int. J. of Material Forming*, 1–26, DOI: 10.1007/s12289-011-1042-y.

[21] Weidig, U., Hübner, K., Steinhoff, K.: Bulk steel products with functionally graded properties produced by differential thermo-mechanical processing, *Steel Research Int.*, 79 (2008) 1, 59–65.